Au/*n*-ZnO rectifying contact fabricated with hydrogen peroxide pretreatment

Q. L. Gu,[1,a)] C. K. Cheung,[1] C. C. Ling,[1,b)] A. M. C. Ng,[1] A. B. Djurišić,[1] L. W. Lu,[1] X. D. Chen,[1] S. Fung,[1] C. D. Beling,[1] and H. C. Ong[2]
[1]*Department of Physics, The University of Hong Kong, Pokfulam Road, Hong Kong, People's Republic of China*
[2]*Department of Physics, Chinese University of Hong Kong, Shatin, Hong Kong, People's Republic of China*

(Received 21 December 2007; accepted 27 February 2008; published online 5 May 2008)

Au contacts were deposited on *n*-type ZnO single crystals with and without hydrogen peroxide pretreatment for the ZnO substrate. The Au/ZnO contacts fabricated on substrates without H_2O_2 pretreatment were Ohmic and those with H_2O_2 pretreatment were rectifying. With an aim of fabricating a good quality Schottky contact, the rectifying property of the Au/ZnO contact was systemically investigated by varying the treatment temperature and duration. The best performing Schottky contact was found to have an ideality factor of 1.15 and a leakage current of $\sim 10^{-7}$ A cm^{-2}. A multispectroscopic study, including scanning electron microscopy, positron annihilation spectroscopy, deep level transient spectroscopy, x-ray photoelectron spectroscopy, and photoluminescence, showed that the H_2O_2 treatment removed the OH impurity and created Zn-vacancy related defects hence decreasing the conductivity of the ZnO surface layer, a condition favorable for forming good Schottky contact. However, the H_2O_2 treatment also resulted in a deterioration of the surface morphology, leading to an increase in the Schottky contact ideality factor and leakage current in the case of nonoptimal treatment time and temperature. © *2008 American Institute of Physics*. [DOI: 10.1063/1.2912827]

I. INTRODUCTION

ZnO is a wide band gap semiconductor material that has attracted widespread attention because of its potential device applications such as optoelectronic and spintronic.[1–3] Although fabricating Schottky contacts is essential for developing ZnO-based devices, making a good quality rectifying contact to ZnO is not trivial. According to the Schottky–Mott model, the barrier height of an ideal Schottky contact, ϕ_b, is given by the difference between the metal work function ϕ_m and the semiconductor electron affinity χ_s, i.e., $\phi_b = \phi_m - \chi_s$. Thus, metals that have a work function larger than the electron affinity of ZnO [4.35 eV (Ref. 4)] would be possible candidates for forming Schottky contacts and the Schottky barrier height increases with the metal work function. Metals such as Pt (ϕ=5.65 eV), Pd (ϕ=5.12 eV), and Au (ϕ =5.10 eV) (Ref. 5) would be able to form Schottky contacts and these would have calculated Schottky barrier heights of 1.30, 0.77, and 0.75 eV, respectively.

Although there were some successes in fabricating rectifying contacts on *n*-type ZnO by using these metals,[6–20] most of these contacts had relatively high values of leakage current and ideality factor. Moreover, the measured Schottky barrier heights were smaller than that predicted by the Schottky–Mott model. In other cases, the metal/ZnO contacts fabricated were found to be Ohmic rather than rectifying. Surface pretreatments such as wet chemical etching (HCl, H_2O_2, etc.), ozone cleaning, and oxygen plasma cleaning were reported to convert the metal/*n*-ZnO from Ohmic to rectifying or to have the effect of improving the rectifying contact property. With a pretreatment in phosphoric acid and hydrochloric acid, rectifying contacts of Au and Pd were made to a *n*-type ZnO crystal by Mead[6] and Neville and Mead.[7] Oh *et al.*[8] studied the Au contact made to a plasma-assisted molecular beam epitaxy grown N-doped ZnO film and their results suggest that a good Schottky characteristic is associated with an increase in the ZnO:N layer resistivity. Nemanich and co-workers[9,10] observed that oxygen plasma pretreatment removes carbon and OH impurities on the ZnO surface, having the effect of improving the quality of the Au/ZnO Schottky contact. Furthermore, it was also concluded that the difference between the experimental and the Schottky–Mott model values of the Schottky barrier height is due to the existence of interface states. The improvement of the Schottky contact quality induced by UV-ozone cleaning was observed by Ip *et al.*[11] and was related to the removal of C contamination. Mosbacker *et al.*[12] observed an Ohmic to rectifying conversion on a Au/ZnO contact after the ZnO substrate was pretreated with remote room temperature oxygen plasma treatment. This was accompanied by the removal of C and OH contamination, a reduction of the green deep level cathodoluminescence signal and an increase in the band bending. Kim *et al.*[13] also observed an Ohmic to rectifying conversion on a Pt/ZnO contact with pretreatment of $(NH_4)S_x$ solution. This was attributed to the formation of a layer with a reduced net carrier concentration, which is possibly related to the formation of a Zn vacancy acceptor or a ZnS interface, hence, resulting in the low conductivity. In a later study, Kim *et al.*[14] studied the Pt/ZnO contacts fabricated with pretreatment of boiling H_2O_2. The H_2O_2 treatment significantly reduced the leakage current of the diode and, at

[a)]Corresponding author. Electronic address: gump423@gmail.com.
[b)]Corresponding author. Electronic address: ccling@hku.hk.

the same time, the deep level emission photoluminescence (PL) signal was also found to be reduced. This was explained in terms of the removal of a donorlike Zn interstitial and oxygen vacancy, hence, the reduction of the free carrier concentration.

The electrical performance of a metal/ZnO contact depends on a number of factors, for example, OH and C contaminations, interface layer, deep level defects, and surface morphology. A multispectroscopic approach has to be adopted so as to obtain a comprehensive picture of the way these mechanisms influence the contact performance. In a recently published short letter,[21] we observed an Ohmic to rectifying conversion on a Au/*n*-ZnO contact pretreated with H_2O_2 and showed that the conversion is associated with the elimination of the OH contamination and the formation of Zn vacancy or the related vacancy cluster. In the present study, the influence of H_2O_2 pretreatment on the Au/*n*-ZnO samples as well as the condition of pretreatment were systemically investigated with a multispectroscopic approach using *I-V* measurement, x-ray photoelectron spectroscopy (XPS), positron annihilation spectroscopy (PAS), scanning electron microscopy (SEM), deep level transient spectroscopy (DLTS), and PL.

II. EXPERIMENTAL

The as-received *n*-type ZnO (0001) single crystal substrate (Cermet, Inc.) had a carrier concentration of 5×10^{16} cm^{-3} and one side polished. The substrates were first cleaned by acetone and ethanol and then rinsed in de-ionized water each for 5 min at room temperature. Ohmic contacts were fabricated by evaporating a large area Al metal disk onto the rough side of the sample. Circular Au contacts with a diameter of 0.5 mm and a thickness of 50 nm were fabricated by thermal evaporation at a background pressure of 10^{-6} Torr with or without H_2O_2 pretreatment. The temperature and duration of the H_2O_2 treatment varied from room temperature to the boiling point of H_2O_2 and from 1 to 30 min, respectively. *I-V* measurements were conducted with a HP 4155A semiconductor parameter analyzer. To investigate the effect of the H_2O_2 treatment on the vacancy type defect in the ZnO substrate, PAS study was carried out by a variable positron beam and an HPGe gamma ray detector system. The HPGe detector had a resolution of full width at half maximum equal to 1.3 keV at the gamma peak of 514 keV. Surface contamination of the ZnO substrate was studied by XPS with a PHI Quantum 2000 XPS/ESCA system, and for deep level information, DLTS measurements were carried out with a Sula DLTS system. For PL measurements, the samples were excited by a 60 mW HeCd (Kimmon) laser and the signal was dispersed by a 0.25 m spectrometer and then captured by an Andor charge-coupled device detector. An Oxford closed cycle He cryostat was used to vary the sample temperature from 10 to 290 K.

III. RESULTS

I-V measurements were performed on the Au/ZnO samples fabricated with different conditions of H_2O_2 pretreatment. For the same condition of treatment, *I-V* measurements were conducted on at least five Au/ZnO contacts fabricated to ensure the results were reproducible and reliable. The *I-V* data of the Au/ZnO sample fabricated on the untreated ZnO substrate are shown in Fig. 1, from which a clear Ohmic behavior can be observed. We have also fabricated the Au contact on the ZnO substrate pretreated with boiling acetone, boiling trichloroethylene, and boiling methanol, and the resulting Au/ZnO was also found to be of Ohmic nature.

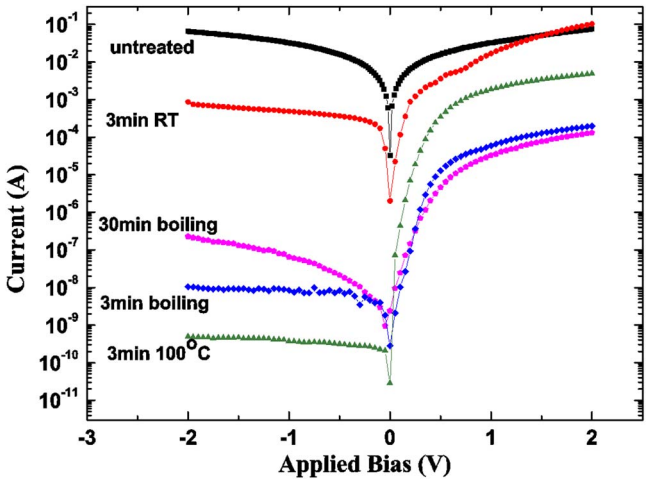

FIG. 1. (Color online) *I-V* data of the Au/ZnO contacts with the ZnO substrates under different H_2O_2 pretreatment conditions.

ZnO substrates were also pretreated with boiling H_2O_2 for different durations (from 1 to 30 min) before the Au contact was deposited. All of the Au/ZnO contacts fabricated with such pretreatments became rectifying and the rectifying properties of the 3 and 30 min boiling H_2O_2 pretreated samples are shown in Fig. 1. The barrier height ϕ_b and the ideality factor n were calculated according to the thermionic emission model, which predicts an *I-V* relation of $I = AA^*T^2 \exp(-q\phi_b/kT)\exp[q(V-IR_S)/nkT]$, where A is the area of the metal contact, A^* is the effective Richardson constant, and R_S is the serial resistance linked to the diode sample. The leakage current observed at $V_R = -1$ V, the calculated ϕ_b, and the ideality factor n of the samples pretreated with boiling H_2O_2 are shown in Table I. The sample pretreated with boiling H_2O_2 for a period of 1–3 min had n

TABLE I. Ideality factors n, barrier height ϕ_n, and leakage current (measured at −1 V reverse bias) of the Au/ZnO contacts fabricated with H_2O_2 pretreatments at different temperatures and with different durations.

	Ideality factor n	Barrier height ϕ_b (eV)	Leakage current at $V_R = -1$ V (A)
		Room temperature	
3 min	2.74	0.35	$\sim 10^{-3}$
		100 °C	
1 min	1.36	0.63	$\sim 10^{-7}$
3 min	1.15	0.63	$\sim 10^{-9}$
30 min	2.25	0.51	$\sim 10^{-8}$
		Boiling	
1 min	1.64	0.60	$\sim 10^{-8}$
3 min	1.67	0.60	$\sim 10^{-8}$
30 min	2.89	0.53	$\sim 10^{-7}$

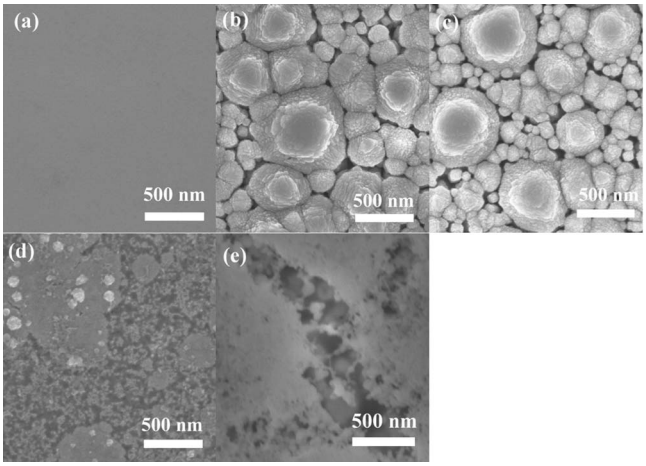

FIG. 2. SEM images of the ZnO samples with different H_2O_2 treatments, namely (a) untreated; (b) 100 °C for 3 min; (c) 100 °C for 30 min; (d) boiling for 3 min; and (e) boiling for 30 min.

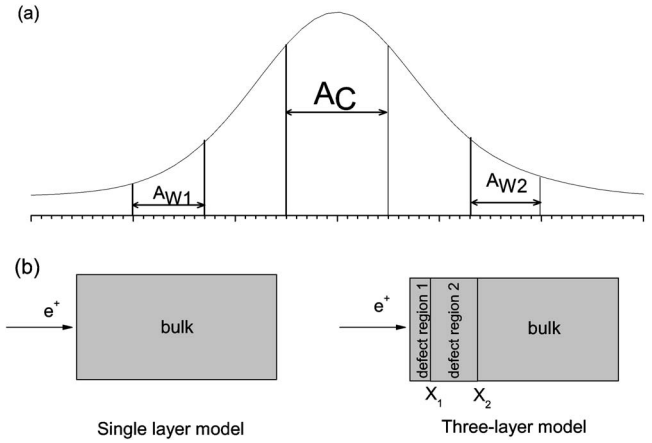

FIG. 3. (a) Definitions of the *S*-parameter and the *W*-parameter for characterizing the lineshape of the annihilation peak. (b) illustrates the one layer and three layer models used to obtain good fitting for the $S(E)$ data of the untreated and the H_2O_2 treated ZnO samples.

~ 1.7, $\phi_b \sim 0.62$, and $I_{\text{leak}} \sim 10^{-8}$ A at $V_R = -1$ V. With a prolonged pretreatment of 30 min, the parameters deteriorated to $n=2.9$, $\phi_b=0.53$ eV, and $I_{\text{leak}}=4\times10^{-7}$ A at $V_R=-1$ V.

With the aim of increasing the barrier height and lowering the ideality factor and the leakage current, we extended the study to Au/ZnO samples fabricated with H_2O_2 pretreatment at room temperature and 100 °C. The parameters of these Schottky contacts are shown in Table I. The samples fabricated with H_2O_2 for 3 min at room temperature was found to be rectifying, but the ideality factor and the leakage current were large [$n>2.5$, $I_{\text{leak}}(V_R=-1\ \text{V}) \sim 10^{-3}$ A]. A significant improvement was found for the samples fabricated with 100 °C H_2O_2 pretreatment. The best performing diode was the one fabricated with H_2O_2 pretreatment for 3 min at 100 °C, which had values of barrier height, ideality factor, and leakage current equal to $\phi_b=0.63$ eV, $n=1.15$, and $I_{\text{leak}}(V_R=-1\ \text{V})=4.2\times10^{-9}$ A, respectively (*I-V* data as shown in Fig. 1). These correspond to a leakage current density of 6×10^{-7} A cm^{-2}.

SEM was used to investigate the morphological influence to the Schottky contact property. The SEM picture of the untreated ZnO sample shown in Fig. 2(a) illustrates a smooth surface. Figure 2(b) shows that the 3 min at 100 °C H_2O_2 treatment increased the ZnO surface roughness and submicron grain structure was found on the surface. The increase of treatment duration to 30 min while keeping the temperature at 100 °C did not induce a significant change to the ZnO surface [compare Figs. 2(b) and 2(c)]. Figures 2(d) and 2(e) show the surface morphology of the ZnO samples treated at the boiling point of H_2O_2 for 3 and 30 min, respectively, for which the surface quality exhibited significant deterioration.

PAS was also used to investigate the effect of the H_2O_2 treatment on the ZnO surface. PAS has been proved to be a useful probe for investigating vacancy type defects in semiconductors.[22,23] Positrons implanted into the solid are thermalized and then undergo diffusion. If neutral or negatively charged vacancy type defects exist, the diffusing positrons, being positive, will be trapped by these defects. The positron in the delocalized bulk state or in the localized defect state will finally annihilate with its surrounding electron and emit a pair of gamma photons. The principle of PAS is that the outgoing annihilation gamma photons carry the information of the electronic environment at which the positron annihilates. In the present study, monoenergetic positrons were implanted into the sample to the desired depth by varying the positron implanting energy up to a value of 30 keV. The electronic environment at different depths was revealed by the Doppler broadening of the annihilation gamma photons, which was parameterized by the *S*-parameter and the *W*-parameter. The *S*-parameter and *W*-parameter are defined as the ratios of the count of a fixed central window [*C*, as shown in Fig. 3(a)] and the count of the pair of fixed windows [W_1+W_2, as shown in Fig. 3(a)] to the total count of the annihilation peak, respectively. The central region and the side windows of the annihilation peak were associated with the events of the positron annihilating with the low momentum valence electron and the high momentum core electron, respectively. As the wave function of a positron in the localized vacancy state has a greater overlap with that of a valance electron as compared to a core electron, a larger measured *S*-parameter indicates that more positrons annihilate in the vacancy state and/or in a larger open volume vacancy type defect.

The *S*-parameter as a function of the positron implanting energy for the ZnO samples with different H_2O_2 treatment conditions (i.e., 3 min at 100 °C, 30 min at 100 °C, and 30 min at boiling H_2O_2) are shown in Fig. 4. The measured *S*-parameter is the weighted contributed from the different annihilating sites, i.e., $S(E)=\Sigma f_i(E)S_i$, where f_i is the fraction of positrons annihilating at the site i and S_i is its characteristic *S*-parameter. The $S(E)$ data were fitted by the source code VEPFIT,[24] for which the dynamic and the annihilation of positrons implanting into the sample were modeled by the equation[22–24]

$$\frac{\partial n(x,t)}{\partial t} = D_+ \frac{\partial^2 n(x,t)}{\partial x^2} - v_d \frac{\partial n(x,t)}{\partial x} - \lambda_{\text{eff}} n(x,t), \qquad (1)$$

where $n(x,t)$ is the positron density at a position x and a time t after the implantation, D_+ is the positron diffusion constant,

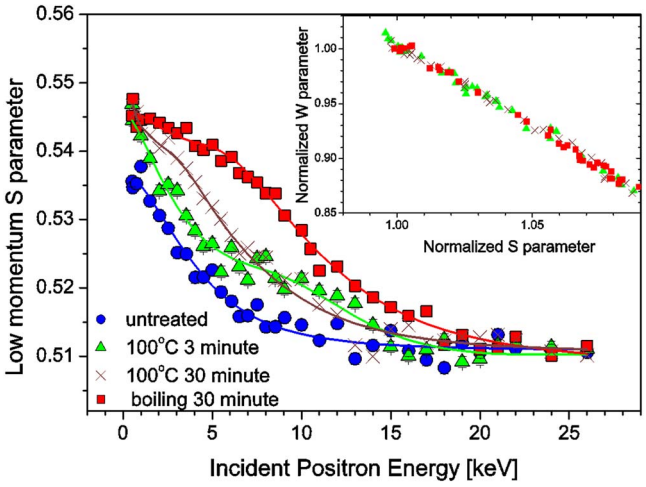

FIG. 4. (Color online) $S(E)$ data for the untreated ZnO sample (blue circles) and for the samples treated with H_2O_2 for 3 min at 100 °C (green triangles), for 30 min at 100 °C (brown crosses), and for 30 min at the boiling point of H_2O_2 (red squares). The inset shows the measured S-parameter plotted against its own W parameter for the H_2O_2 treated sample, clearly yielding a straight line.

v_d is the electric field dependent positron drift velocity, $\lambda_{\text{eff}} = 1/\tau_b + \kappa(x)$ is the effective positron annihilation rate, τ_b is the positron bulk lifetime, and κ is the positron trapping rate into the vacancy. The effective positron diffusion length is given by[22–24]

$$L_{+,\text{eff}} = (D_+/\lambda_{\text{eff}})^{1/2} \tag{2}$$

for zero electric field. The positron implantation depth profile is given by the Makhov equation originally used for electron implantation,[25] i.e., $P(x,E) = (mx^{m-1}/x_0^m)\exp[-(x/x_0)^m]$, with $x_0 = \bar{x}/\Gamma(1+1/m)$, where Γ is the gamma function and $\bar{x}$ is the mean implantation depth given by $\bar{x} = AE^n$. The empirical values of the parameters are generally accepted as $m=2$, $n=1.6$, and $A = 400/\rho$ Å keV^{-n}, where ρ is the sample mass density in the unit of g cm^{-3}. The sample was considered to be in a layered structure [as shown in Fig. 3(b)] and each of the layers has its own effective positron diffusion length L_+ and characteristic S-parameter. The fraction of positron annihilating at the different layers can thus be found by solving Eq. (1).

Referring to the $S(E)$ of different samples, as shown in Fig. 4, a one layer model [as shown in Fig. 3(b)] resulted in a good fit to the untreated sample, but a three layer model [as shown in Fig. 3(b)] was needed for the H_2O_2 treated samples. The fitted curves are denoted by the solid lines in Fig. 4. The fitted S-parameters and the effective positron diffusion lengths for each of the layers of the samples are shown in Table II. The applicability of the one layer model to the untreated sample $S(E)$ data implied that the untreated sample was of a homogeneous bulk structure having an effective positron diffusion of 72 nm and an S-parameter of 0.5109 (fitted results as shown in Table II). For the H_2O_2 treated samples, the existence of the two extra layers having a relatively high S-parameter and a low effective diffusion length on top of the bulk revealed that the H_2O_2 treatment induced the formation of vacancy type defects in the regions.

In order to investigate the nature of the vacancy type defects induced during the H_2O_2 treatment, the S-parameter of each of the annihilation events for the H_2O_2 treated samples was plotted against its own W-parameter, as shown in the inset of Fig. 4. In general, the measured S and W parameters are given by

$$S = \left(1 - \sum_{i=1}^{N} f_{di}\right) S_b + \sum_{i=1}^{N} f_{di} S_{di} \tag{3}$$

and

$$W = \left(1 - \sum_{i=1}^{N} f_{di}\right) W_b + \sum_{i=1}^{N} f_{di} W_{di}, \tag{4}$$

where S_b and W_b are the S and the W parameters of the bulk, respectively, and f_{di} is the fraction of positron annihilating in the defect state i ($i=1$ to N), with the corresponding characteristic S and W parameters S_{di} and W_{di}. It can easily be derived from Eqs. (3) that

TABLE II. Fitted results of the *SE* data shown in Fig. 4. The indices S, 1, 2, and B in the S-parameter and the diffusion length L denote the surface, the first layer, the second layer, and the bulk, respectively, while X_1 and X_2 are the boundary positions of the first and the second layers, respectively. C is the concentration of the corresponding vacancy type defect induced by the H_2O_2 treatment with the value of the positron trapping coefficient taken to be $\mu = 10^{15}$ s^{-1}.

	Surface	First layer	Second layer	Bulk
Untreated	$S_S = 0.5373$	NA	NA	$S_B = 0.5109$ $L_B = 72$ nm
3 min at 100 °C	$S_S = 0.5453$	$S_1 = 0.5224$ $L_1 = 35$ nm $X_1 = 56$ nm $C_1 = 3.0 \times 10^{17}$ cm^{-3}	$S_2 = 0.5212$ $L_2 = 48$ nm $X_2 = 393$ nm $C_2 = 2.0 \times 10^{17}$ cm^{-3}	$S_B = 0.5092$ $L_B = 70$ nm
30 min at 100 °C	$S_S = 0.5437$	$S_1 = 0.5389$ $L_1 = 30$ nm $X_1 = 92$ nm $C_1 = 3.4 \times 10^{17}$ cm^{-3}	$S_2 = 0.5183$ $L_2 = 42$ nm $X_2 = 290$ nm $C_2 = 2.4 \times 10^{17}$ cm^{-3}	$S_B = 0.5104$ $L_B = 72$ nm
30 min at Boiling	$S_S = 0.5465$	$S_1 = 0.5401$ $L_1 = 29$ nm $X_1 = 223$ nm $C_1 = 3.5 \times 10^{17}$ cm^{-3}	$S_2 = 0.5202$ $L_2 = 37$ nm $X_2 = 422$ nm $C_2 = 2.9 \times 10^{17}$ cm^{-3}	$S_B = 0.5086$ $L_B = 72$ nm

$$\frac{S-S_b}{W-W_b}=\frac{\left(\sum_{i=1}^{N} f_{di}S_{di}\right)-\left(\sum_{i=1}^{N} f_{di}S_b\right)}{\left(\sum_{i=1}^{N} f_{di}W_{di}\right)-\left(\sum_{i=1}^{N} f_{di}W_b\right)}. \quad (5)$$

Equation (5) shows that, in general, if $N>1$, $(S-S_b)/(W-W_b)$ is not a constant. However, if there is only a single type of defect, Eq. (5) would be reduced to

$$\frac{S-S_b}{W-W_b}=\frac{S_d-S_b}{W_d-W_b}, \quad (6)$$

which is a constant and, thus. the *SW* plot would be of a straight line. The straight line observed in the inset of Fig. 4 shows that the vacancy type defects induced by the H_2O_2 treatment were the same type irrespective of the treatment temperature and duration. Positron trapping into Zn vacancy related defects and vacancy cluster was observed in *n*-type ZnO.[26–30] Positron annihilation does not occur in the O vacancy at room temperature because of its low binding energy.[26–30] This implies that the vacancy type defect induced by the H_2O_2 treatment observed in the present study should be Zn vacancy or vacancy cluster.

As the measured effective positron diffusion length is limited by positron trapping into vacancy, as shown in Eq. (2), [i.e., $L_+^2=D_+/(\tau_b^{-1}+\kappa)$], the drop in the measured L_+ after the H_2O_2 treatment is related to the concentration of the induced vacancy type defect by

$$\frac{2dL_+}{L_+}=\frac{-d\kappa}{\lambda_{\text{eff}}}=\frac{\mu C}{\lambda_{\text{eff}}}, \quad (7)$$

where μ and C are the specific coefficients of positron trapping into the vacancy and the vacancy concentration. The value of μ was 10^{15}–10^{16} s^{-1} and λ_{eff} of the untreated sample was found to be $(166\ \text{ps})^{-1}$ by the positron lifetime measurement. The concentration of the induced vacancy type defects was thus in the range of 10^{17}–10^{18} cm^{-3} as calculated from the fitted L_+ values, as shown in Table II.

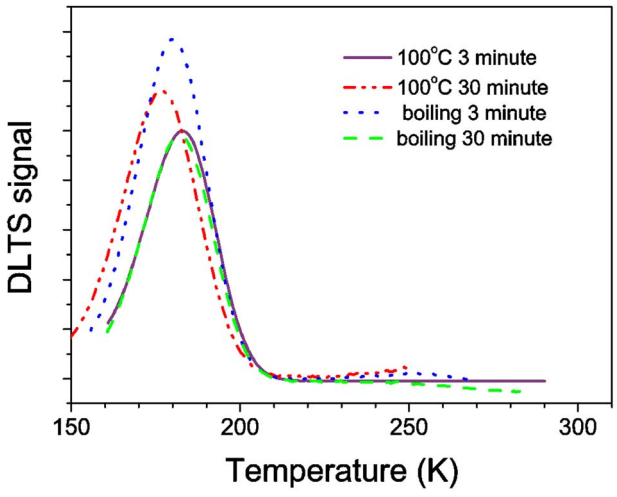

FIG. 5. (Color online) DLTS spectra obtained from the Au/ZnO Schottky contacts with the substrates pretreated with H_2O_2 for 3 min at 100 °C, for 30 min at 100 °C, for 3 min at the boiling point of H_2O_2, and for 30 min at the boiling point of H_2O_2.

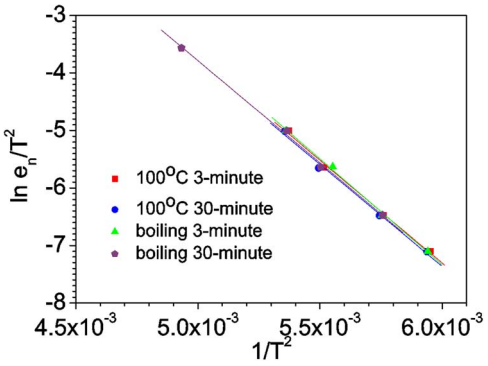

FIG. 6. (Color online) Arrhenius plots of deep levels as found in the Au/ZnO samples with the substrates pretreated with H_2O_2 for 3 min at 100 °C, for 30 min at 100 °C, for 3 min at the boiling point of H_2O_2, and for 30 min at the boiling point of H_2O_2.

We have also carried out DLTS study for the rectifying diode fabricated with H_2O_2 pretreatment under different conditions (i.e., 3 min at 100 °C, 30 min at 100 °C, 3 min at boiling, and 30 min at boiling) and the DLTS spectra are shown in Fig. 5. A single peak at about 180 K was observed in the spectra of all of the samples irrespective of the treatment condition. The corresponding Arrhenius plots of these samples, which are shown in Fig. 6, indicate that they were associated with the same defect. The values of the activation energy and the capture cross section were obtained by the relation $e_n/T^2=\gamma_n\sigma_n \exp[-E_a/kT]$, where e_n is the rate of emission from the deep level to the conduction band, γ_n is a constant, σ_n is the capture cross section, and E_a is the defect activation energy. The activation energy, the concentration, and the capture cross section of the deep level defects found in the samples with different H_2O_2 treatments are shown in Table III. The deep level found in all of these samples should be identical as they have the same activation energy (0.31 eV) and capture cross section ($\sim 10^{-16}$ cm^2). Moreover, it was observed that the concentration of this deep level found in all of the samples was independent of the H_2O_2 treatment condition ($\sim 10^{15}$ cm^{-3}). Deep level defects with similar activation energies (i.e., 0.29 and 0.31 eV) were reported in as-grown *n*-type ZnO single crystals.[15,31,32] In particular, in an earlier study,[32] nitrogen was implanted into the *n*-ZnO single crystal, whereas the ZnO substrates were grown by an identical method and obtained from the same company and had the similar free carrier concentration as the ones of the present study. DLTS study on the resulting *p-n* junction re-

TABLE III. Activation energies, concentrations, and capture cross sections of the deep level defect found in the samples with treatments of 3 min at 100 °C, 30 min at 100 °C, 3 min at the boiling point of H_2O_2, and 30 min at the boiling point of H_2O_2.

	Activation energy E_a (eV)	Defect concentration C_n (cm^{-3})	Capture cross section σ_n (cm^2)
3 min at 100 °C	0.309	0.9×10^{15}	4.3×10^{-16}
30 min at 100 °C	0.306	1.0×10^{15}	3.3×10^{-16}
3 min at boiling	0.317	1.2×10^{15}	5.0×10^{-16}
30 min at boiling	0.307	0.9×10^{15}	3.7×10^{-16}

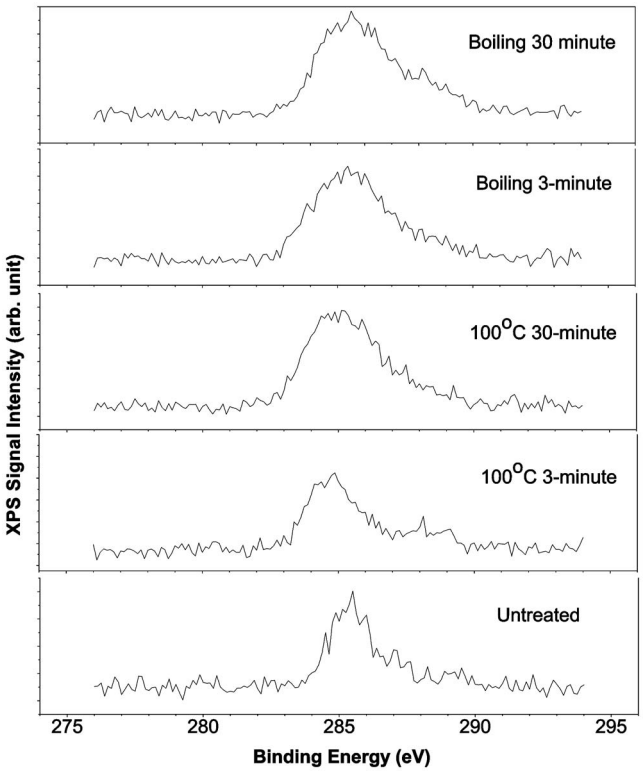

FIG. 7. C 1*s* signal as found in XPS spectra obtained from the untreated ZnO sample and from the samples treated with H_2O_2 for 3 min at 100 °C, for 30 min at 100 °C, for 3 min at the boiling point of H_2O_2, and for 30 min at the boiling point of H_2O_2.

vealed the deep level E3 having an exact activation energy (i.e., 0.31 eV) as found here. Moreover, the reported concentration and the capture cross section of the E3 were within the range of 10^{15} cm^{-3} and 10^{-16} cm^2, which are also similar to the present results. As the same deep level with the same concentration was found in all of the present Schottky contacts irrespective of the H_2O_2 treatment condition and also in the *p-n* junction fabricated by *N* implantation, this deep level defect should not be a product induced by the fabrication process, such as H_2O_2 treatment or nitrogen implantation, but should be present in the as-grown pressurized melted grown ZnO single crystal obtained from Cermet, Inc. This implies that this deep level defect did not play an important role in determining the Au/ZnO contact electrical property in the present study.

XPS was employed to study the surface chemical condition dependence on the different H_2O_2 treatments. XPS signals of 285, 531, and 1022 eV were identified at the surface of the untreated ZnO sample and they were attributed to carbon (C 1*s*), oxygen (O 1*s*), and zinc (Zn $2p_{2/3}$). The carbon signal disappeared after Ar sputtering corresponding to a thickness of 50 Å, implying that the carbon signal originated from the carbon impurity on the sample surface. The dependence of the C signal on the H_2O_2 treatment are shown in Fig. 7, indicating that the C impurity persisted after different H_2O_2 treatment conditions. This observation implied that in the present study, the carbon impurity on the ZnO surface did not play a significant role in determining the Au/ZnO contact

TABLE IV. Atomic ratios of O and OH and also the Zn:O ratio on the surfaces of the ZnO substrate for different conditions of H_2O_2 treatments as obtained from the XPS measurements.

	O	OH	Zn:O ratio
Nontreated	20.9%	26.1%	1.86
3 min at 100 °C	55.2%	1.3%	0.40
30 min at 100 °C	49.4%	6.2%	0.29
3 min at boiling	40.4%	14.6%	0.27
30 min at boiling	36.5%	20.9%	0.27

electrical property. Identical observations were also made in the Auger electron spectroscopic measurements on similar samples.[33]

For the O signal, two peaks were required to obtain a good fit to the spectra, with the fitted results and the curves shown in Table IV and Fig. 8. The average binding energies of the two O-related peaks were 531.3 and 532.8 keV. A similar behavior was observed for different types of ZnO surfaces and the two peaks were associated with O and OH.[9,10,12] It was obvious from Fig. 8 and Table IV that the H_2O_2 treatment would have the effect of reducing the OH signal intensity. The atomic Zn:O ratio was calculated and tabulated in Table IV. It was observed that with the H_2O_2 treatment, the sample surface changed from being Zn rich (Zn:O=1.86 for the untreated sample) to being O rich (Zn:O=0.27–0.40, depending on the treatment condition).

The optical properties of the untreated and H_2O_2 pretreated ZnO substrates were investigated by low-temperature PL carried out at 10 K. As shown in Fig. 9, the spectra are

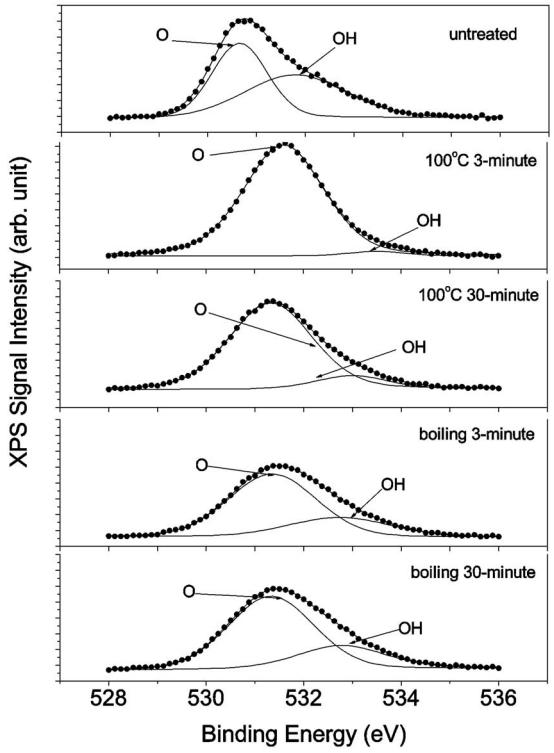

FIG. 8. O 1*s* signal as found in the XPS spectra obtained from the untreated ZnO sample and from the samples treated with H_2O_2 for 3 min at 100 °C, for 30 min at 100 °C, for 3 min at the boiling point of H_2O_2, and for 30 min at the boiling point of H_2O_2.

dominated by strong near band-edge emissions that originated from neutral-donor bound exciton (D^0X) and weaker deep level defect emission. It is evident that the untreated sample has the strongest band-edge emission and the weakest deep level emission. After the 3 min at 100 °C H_2O_2 treatment, the intensity of the deep level emission remains almost unchanged, but the band-edge emission is significantly weakened. The intensity of the deep level defect emission significantly increases in the sample pretreated with H_2O_2 for 30 min at the boiling point and that of the band-edge emission further decreases. All of the above results suggest that the surface H_2O_2 treatment on the ZnO substrates decreased the intensity of the band-edge emission and increased that of the defect emission. The spectra obtained in the range of deep level emission are presented in the inset of Fig. 9. It should be noted that interference patterns can be observed in the spectrum of 30 min boiling-H_2O_2 treated ZnO sample. This indicates that the top surface layer of the sample probably has different reflection coefficients from the lower layer. The present result suggests that the deep level defect related to the observed defect emission is not the origin of the Ohmic behavior of the untreated Au/ZnO contact.

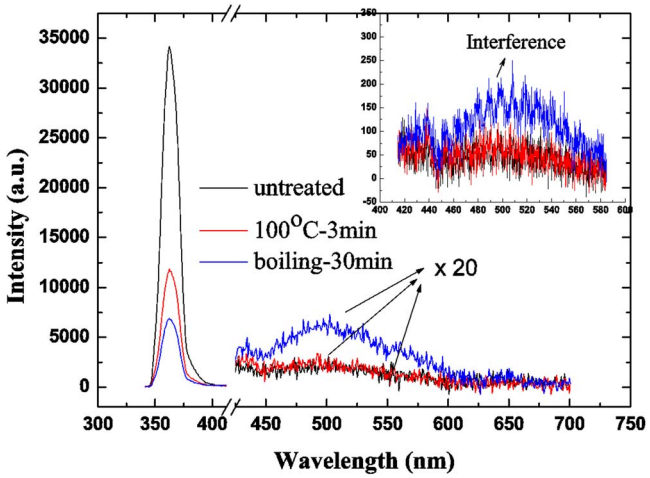

FIG. 9. (Color online) PL spectra obtained at 10 K from the surface of the untreated ZnO substrate and those of the ZnO substrates pretreated with H_2O_2 for 3 min at 100 °C and for 30 min at the boiling point of H_2O_2. The inset presents expanded spectra for the deep level emissions involved.

IV. DISCUSSION AND CONCLUSION

From Fig. 1, it can be seen that the 3 min room temperature treatment converts the *IV* behavior from a symmetric Ohmic behavior to an asymmetric rectifying one ($I_{leak} \sim 10^{-3}$ A). Increasing the treatment temperature to 100 °C but fixing the treatment duration as 3 min would yield the best performing diode, which had $I_{leak} \sim 10^{-9}$ A, and further increasing the temperature to that of boiling H_2O_2 would worsen the I_{leak} to $\sim 10^{-8}$ A. Increasing the treatment duration to 30 min in boiling H_2O_2 would further increase the I_{leak} to 10^{-7} A. The SEM images (Fig. 2) showed that the untreated sample surface had the best morphology among the others. H_2O_2 treatment at 100 °C would induce submicron grain structure. In previous studies of metal/ZnO contact, it was reported that a good Schottky contact was associated with a good sample surface morphology. The observation in the present study revealed that the ZnO substrate morphology was not the only factor determining the fabricated Au/ZnO diode as the sample fabricated with the untreated ZnO surface was found to be Ohmic. On the other hand, although the 3 min at 100 °C H_2O_2 treatment increased the surface roughness and induced submicron grain structure, the resulting Au/ZnO sample was the best performing Schottky contact. The 3 and the 30 min boiling H_2O_2 treatments on the ZnO substrate resulted in very poor morphology. Despite this, the Au/ZnO contact fabricated from this substrate was still rectifying though the leakage current and the ideality factor were large. The high values of the ideality factor and the leakage current could be understood from the deterioration of the morphology. Moreover, the low-temperature PL also indicated the increase of deep level defect emission after the H_2O_2 treatment. As the bad morphology and the deep level defects have been associated with poor rectifying property of Schottky contact, there is another mechanism prohibiting the Au/ZnO sample fabricated from the untreated substrate from having good rectifying behavior. This mechanism can be removed by H_2O_2 treatment.

The results of the XPS study, as shown in Fig. 8 and Table IV, indicate that the surface OH intensity dropped after the H_2O_2 treatment. It was also found from the present data that the best performing Au/ZnO contact fabricated from the 3 min at 100 °C treated substrate was the one with the lowest OH intensity. However, it was also interesting to note that the OH intensity did not drop further but increased after treatment with more vigorous conditions (i.e., higher temperature or longer duration). The reason for this observation is not understood and requires further investigation. In previous studies conducted by Polyakov *et al.*,[16] Oh *et al.*,[8] Coppa *et al.*,[8] and Kim *et al.*,[14] C and OH impurities on ZnO surface were removed after surface treatments such as ozone and plasma cleaning. After these surface treatments, improvements on the metal/ZnO contact property or Ohmic to rectifying conversion were observed. It was further argued that the C and OH contaminations were possible causes for the difficulty in fabricating good performing metal/ZnO Schottky contacts. In the present study, it was observed that the C impurity on the ZnO surface could not be removed by the H_2O_2 treatments. As the Au/ZnO contacts fabricated with the substrates having such C surface contamination still have a good rectifying property (such as the sample fabricated from the 3 min at 100 °C treated substrate), it is thus plausible to conclude that the improvement in the contact rectifying property is related to the removal of OH rather than the C impurity. As the presence of the OH is known to lead to the formation of an accumulation layer having a high conductivity on the ZnO surface,[34–36] the presence of such an accumulation layer would undoubtedly prevent the fabrication of a good quality rectifying contact on the ZnO surface.

The results of the present PAS study reveal the creation of Zn-vacancy defects up to the concentration of 10^{17} cm^{-3} at the substrate surface upon the H_2O_2 treatment. The Zn

vacancy in ZnO is an acceptor and the formation of this defect would have a compensation effect, thus reducing the surface free carrier concentration.

In conclusion, we have successfully fabricated good performing rectifying Au/ZnO contacts by pretreating the ZnO substrate with H_2O_2. The H_2O_2 pre-treatment has the effects of reducing the OH impurity and inducing the formation of Zn vacancy acceptor on the substrate surface. This induced Ohmic to rectifying conversion behavior in the Au/ZnO contact can thus be understood in terms of the suppression of the free carrier concentration at the surface region of the ZnO substrate.

ACKNOWLEDGMENTS

We wish to acknowledge financial support from the CERG, RGC, HKSAR (Grant No. 7037/06) and the Seed Funding Program for Basic Research, HKU (Project Code 200611159143); the positron beam facility was financially sponsored by the University Development Fund, HKU.

[1]Ü. Özgür, Ya. I. Alivov, C. Liu, A. Teke, M. A. Reshchikov, S. Doğan, V. Avrutin, S.-J. Cho, and H. Morkoç, J. Appl. Phys. **98**, 041301 (2005).
[2]S. J. Pearton, D. P. Norton, K. Ip, Y. W. Heo, and T. Steiner, Prog. Mater. Sci. **50**, 293 (2005).
[3]D. C. Look, Mater. Sci. Eng., B **80**, 383 (2001).
[4]J. A. Aranovich, D. G. Golmayo, A. L. Fahrenbruch, and R. H. Bube, J. Appl. Phys. **51**, 4260 (1980).
[5]E. H. Rhoderick and R. H. Williams, *Monographs in Electrical and Electronic Engineering* (Oxford Science, Oxford, 1988), Vol. 19, p. 48.
[6]C. A. Mead, Phys. Lett. **18**, 218 (1965).
[7]C. Neville and C. A. Mead, J. Appl. Phys. **41**, 3795 (1970).
[8]D. C. Oh, J. J. Kim, H. Makino, T. Hanada, M. W. Cho, T. Yao, and H. J. Ko, Appl. Phys. Lett. **86**, 042110 (2005).
[9]B. J. Coppa, R. F. Davis, and R. J. Nemanich, Appl. Phys. Lett. **82**, 400 (2003).
[10]B. J. Coppa, C. C. Fulton, P. J. Hartlieb, R. F. Davis, B. J. Rodriguez, B. J. Shields, and R. J. Nemanich, J. Appl. Phys. **95**, 5836 (2004).
[11]K. Ip, B. P. Gila, A. H. Onstine, E. S. Lambers, Y. W. Heo, K. H. Baik, D. P. Norton, S. J. Pearton, S. Kim, J. R. LaRoche, and F. Ren, Appl. Phys. Lett. **84**, 5133 (2004).
[12]H. L. Mosbacker, Y. M. Strzhemechny, B. D. White, P. E. Smith, D. C. Look, D. C. Reynolds, C. W. Litton, and L. J. Brillson, Appl. Phys. Lett. **87**, 012102 (2005).
[13]S. H. Kim, H. K. Kim, and T. Y. Seong, Appl. Phys. Lett. **86**, 022101 (2005).
[14]S. H. Kim, H. K. Kim, and T. Y. Seong, Appl. Phys. Lett. **86**, 112101 (2005).
[15]F. D. Auret, S. A. Goodman, M. Hayes, M. J. Legodi, H. A. van Laarhoven, and D. C. Look, Appl. Phys. Lett. **79**, 3074 (2001).
[16]A. Y. Polyakov, N. B. Smirnov, E. A. Kozhukhova, V. I. Vdovin, K. Ip, Y. W. Heo, D. P. Norton, and S. J. Pearton, Appl. Phys. Lett. **83**, 1575 (2003).
[17]G. Yuan, Z. Ye, L. Zhu, J. Huang, Q. Qian, and B. Zhao, J. Cryst. Growth **268**, 169 (2004).
[18]H. Sheng, S. Muthukumar, N. W. Emanetoglu, and Y. Lu, Appl. Phys. Lett. **80**, 2132 (2002).
[19]H. von Wenckstern, E. M. Kaidashev, M. Lorenz, H. Hochmuth, G. Biehne, J. Lenzner, V. Gottschalch, R. Pickenhain, and M. Grundmann, Appl. Phys. Lett. **84**, 79 (2004).
[20]C. Weichsel, O. Pagni, and A. W. R. Leitch, Semicond. Sci. Technol. **20**, 840 (2005).
[21]Q. L. Gu, C. C. Ling, X. D. Chen, C. K. Cheng, A. M. C. Ng, C. D. Beling, S. Fung, A. B. Djurišić, L. W. Lu, G. Brauer, and H. C. Ong, Appl. Phys. Lett. **90**, 122101 (2007).
[22][REMOVED IF= FIELD]*Positron Beams and Their Applications*, edited by P. Coleman (World Scientific, Singapore, 2000).
[23]P. J. Schultz and K. G. Lynn, Rev. Mod. Phys. **60**, 701 (1988).
[24]A. van Veen, H. Schut, J. de Vries, R. A. Hakvoot, and M. R. Ijpma, AIP Conf. Proc. **218**, 171 (1990).
[25]A. F. Makhov, Sov. Phys. Solid State **2**, 1934 (1961).
[26]G. Brauer, W. Anwand, W. Skorupa, J. Kuriplach, O. Melikhova, and C. Moisson, Phys. Rev. B **74**, 045208 (2006).
[27]F. Tuomisto, V. Ranki, K. Saarinen, and D. C. Look, Phys. Rev. Lett. **91**, 205502 (2003).
[28]S. Koida, S. F. Chichibu, A. Uedono, A. Tsukazaki, M. Kawasaki, T. Sota, Y. Segawa, and H. Koinuma, Appl. Phys. Lett. **82**, 532 (2003).
[29]S. Brunner, W. Puff, A. G. Balogh, and P. Mascher, Mater. Sci. Forum **363–365**, 141 (2001).
[30]Z. Q. Chen, M. Maekawa, S. Yamamoto, A. Kawasuso, X. L. Yuan, T. Sekiguchi, R. Suzuki, and T. Ohdaira, Phys. Rev. B **69**, 035210 (2004).
[31]J. C. Simpson and J. F. Cordaro, J. Appl. Phys. **63**, 1781 (1988).
[32]H. von Wenckstern, R. Pickerhain, H. Schmidt, M. Brandt, G. Biehne, M. Lorenz, M. Grundmann, and G. Brauer, Appl. Phys. Lett. **89**, 092122 (2006).
[33]X. D. Chen, C. C. Ling, G. Brauer, W. Anwand, W. Skorupa, and A. B. Djurišić, presented in the 13th International Conference on Positron Annihilation, Hamilton, Canada, 23–28 July 2006 (unpublished).
[34]H. Moormann, D. Kohl, and G. Heiland, Surf. Sci. **100**, 302 (1980).
[35]G. Heiland and P. Kunstamann, Surf. Sci. **13**, 72 (1969).
[36]C. M. Nakagawa and H. Mistsudo, Surf. Sci. **175**, 157 (1986).